RESEARCHERID
THOMSON REUTERS

[Borquez* *et al.*, 7(6): June, 2018]
IC™ Value: 3.00

ISSN: 2277-9655
Impact Factor: 5.164
CODEN: IJESS7

IJESRT

INTERNATIONAL JOURNAL OF ENGINEERING SCIENCES & RESEARCH TECHNOLOGY

IMPLEMENTATION AND EVALUATION OF A SEAWATER DESALINATION PILOT SYSTEM USING TWO-STAGE NANOFILTRATION

Rodrigo Bórquez[*1], Javier Ferrer[2], Catalina Vargas[3]

[*] Chemical Engineering Department, Universidad de Concepción, Chile

[2] Water Resources Department, Universidad de Concepción, Chile

DOI: 10.5281/zenodo.1283118

ABSTRACT

A seawater desalination pilot system using a two-stage nanofiltration membrane (NF90) was designed, implemented, and evaluated. In the first stage (at a laboratory scale), the permeate flux of the NF90 membrane was 39.7 L/(m^2 h), while total dissolved solids rejection reached 93.6% at a transmembrane pressure of 37 bar. In the second stage, the membrane achieved a salt rejection of 99.9% and permeate flux of 72.5 L/(m^2 h) at 16 bar. The pilot system showed a similar behavior operating at 40 and 15 bar in both stages; permeate recovery was 21.0 L/(m^2 h) and 51.3 L/(m^2 h) in the first and second stage, respectively. As the quality of water obtained in the first stage was satisfactory, it was mixed with water from the second stage, resulting in safe drinking water that conforms to local and international standards. The system can be used to treat different types of brackish water and be coupled with renewable energies. It can provide potable water at a cost of US $ 0.75 / m3, which is a competitive price considering the small size of the system. At present, this pilot system supplies drinking water to a coastal village of Chile.

KEYWORDS: Desalination, nanofiltration, pilot system, drinking water.

I. INTRODUCTION

Lack of water resources for consumption and industrial use is one of the greatest concerns worldwide. The Middle East and, North of Africa (MENA) is already the most water stressed region in the world, while water security has also become a key issue in North America and Australia as a result of population and economic growth, and climate change [1]. According to the United Nations Educational, Scientific, and Cultural Organization (UNESCO), it has been estimated that two-thirds of the world's population will be living under water stress by 2025 [2]. Methods such as seawater desalination can be used to solve this problem. In fact, desalinated water production has grown rapidly in the past decade, especially in arid coastal zones. The total installed capacity increased by 57% annually between 2008 and 2013, achieving a production level of 80 million m^3/day of water in 2013. According to the International Desalination Association (IDA), there were around 16,000 desalination plants in operation in 150 countries by 2015, producing 90 million m^3/day of desalinated water [3, 4]. Desalination costs have dropped by 50% in recent decades as a result of the development of new and modified membranes, and the implementation of energy recovery systems. which make membrane technology cost-effective compared to other alternatives [5].

At present, the desalination industry is dominated by reverse osmosis (RO) [6]. This membrane based process exceeds the installed capacity of thermal systems (MSF and MED), which are widely used in the Gulf Cooperation Council (GCC) and the MENA. Great efforts have been made to improve efficiency and reduce energy consumption in desalination processes. However, implementation of seawater desalination systems continues to be a challenge due to the operating costs associated with high operating pressures and fouling by divalent ions [7].

Nanofiltration (NF) is considered as an effective membrane process [8-10]. The pore sizes of NF lie between those of RO and UF membranes. NF operates at lower transmembrane pressures (TPs), generates greater permeate fluxes, and requires lower investment costs as compared to RO. Additionally, NF has a high removal (high rejection) of divalent ions, especially anions [11]. Due to all these characteristics, NF is gaining importance in seawater desalination [12]. There are some alternatives based on the use of NF for seawater desalination, such as the two-stage nanofiltration process developed by Gouellec [13]. This technique reduces energy consumption by

ISSN: 2277-9655
Impact Factor: 5.164
CODEN: IJESS7

up to 20–30% as compared to RO. It was reported to be applied at a production scale in Long Beach (USA), obtaining a flow of 1135 m^3/day of drinking water. Transmembrane pressure (TP) of each NF stage significantly affects the generated water flow and total dissolved solids (TDS) of the water within the operational parameters considered in this system [14].

NF is a very complex process that depends on micro-hydrodynamics and interfacial events that take place on the membrane surface and inside the nanopores. In this process, a combination of steric, Donnan, dielectric, and transport effects causes the rejection. The dissociation of ionizable groups on the membrane surface and inside the pores generates the charge in the membrane [15]. The dissociation of these surface groups strongly depends on the pH of the contact solution; the membrane can exhibit an isoelectric point at a given pH when membrane surface chemistry is amphoteric [16]. NF membranes also have a weak ion-exchange capacity. Therefore, some ions can be adsorbed on the membrane surface, thus causing a slight modification in the surface charge [17]. Electrostatic repulsion or attraction occurs according to ion valence and the charge of the membrane.

Membrane fouling is a key factor affecting both competitiveness and effectiveness of the process in terms of costs. Fouling can cause negative effects, such as flux decrease (productivity loss), increased operating costs due to increased energy demand, increased membrane maintenance and cleaning, excessive chemical use, and even reduced membrane lifetime. Therefore, effective fouling control and mitigation are crucial to reduce these adverse effects. Removing the largest possible amount of water contaminants associated with the phenomenon before the NF operation is a widely used strategy to prevent fouling. Moreover, microfiltration (MF) is considered as one of the most frequently applied operations, even though there are different pretreatments in NF and RO operations [18].

The objective of this study was to design, implement and evaluate a seawater desalination system using two-stage nanofiltration. The system was designed (Chilean Patent Nº 52.855, 2013-2033) to be used in the coastal area of Chile, and then tested at a pilot-plant scale before its final implementation. It can be described as an adaptable modular system, which allows for easy transport and operational flexibility. It can be used for both seawater and brackish water, which allows generating not only drinking water, but also water for a range of industrial and domestic purposes. As it is a flexible modular system, it can be fully powered with renewable energy. At present, the system supplies drinking water to a coastal village located in south of Chile.

In order to develop the pilot system, the experiment was initially carried out at a laboratory scale. Optimal operating conditions for seawater desalination were determined. This included the determination of the best qualities of the obtained permeate, final salt concentration, and permeate flux density. This system was used to demonstrate the technical feasibility of using seawater nanofiltration for producing drinking water that conforms to local regulations (NCh.409) [19], and guidelines of the World Health Organization (WHO).

The implementation of seawater desalination processes to produce drinking water is of special interest in Chile due to water scarcity in the dry areas of the country and incidence of droughts. Chile has some of the driest areas in the world. Human activities in these areas require large volumes of water, resulting in high water scarcity that has led to environmental degradation, conflicts and reduced industrial productivity [20]. While the North of Chile is characterized for being a desert area that uses large volumes of water for mining operations, the central zone of Chile, which concentrates most of the cities and the agricultural activity of the country, has been under strong drought conditions. In fact, droughts have affected the country on a fairly regular basis, but these have become more frequent in recent years. The recent (2010-2015) multi-year, regional-scale dry event has been referred to as the Central Chile mega drought [21].

II. MATERIALS AND METHODS

Characterization of the seawater used in the tests

The coastal area of the Bio Bio Region, Chile, was used to supply seawater for the tests in this study. The characteristics of the seawater used in the tests are shown in Table 1.

Table 1. Composition of the seawater used in the tests.

Parameter	Unit	Result
pH	-	7.4 ±0.35
Conductivity	µS/cm	51000 ±200
Hardness	mg $CaCO_3$/L	8137 ±20
TSS	mg/L	13 ±1.5
Chloride	mg/L	19350 ±425

ISSN: 2277-9655
Impact Factor: 5.164
CODEN: IJESS7

Sulfate	mg/L	2719 ±416
Nitrate	mg/L	<0.023
Boron	mg/L	5.48 ±0.07
Sodium	mg/L	11080 ±28
Magnesium	mg/L	1672 ±5.4
Calcium	mg/L	502 ±0.6
Potassium	mg/L	516 ±2.2
Ammonium	µg/L	130 ±14
Carbonate	mg/L	<3.0

In Table 1, all analyses were carried out according to standard methods [22] in triplicate.

Equipment used at the laboratory scale

Microfiltration (MF) system

A Kerasep 1-µm MF membrane from Rhodia Orelis was used. It is a tubular, multichannel, Al_2O_3/TiO_2-supported membrane with an active surface of ZrO_2–TiO_2. The unit was operated in batch mode to produce microfiltered water according to the method of Afonso, et al. [23]. The applied TP was 3 bar; feed flow through the membrane was 1.8 m^3/h, and temperature was regulated at 15 °C by circulation of cold water and the heat exchanger (Figure 1).

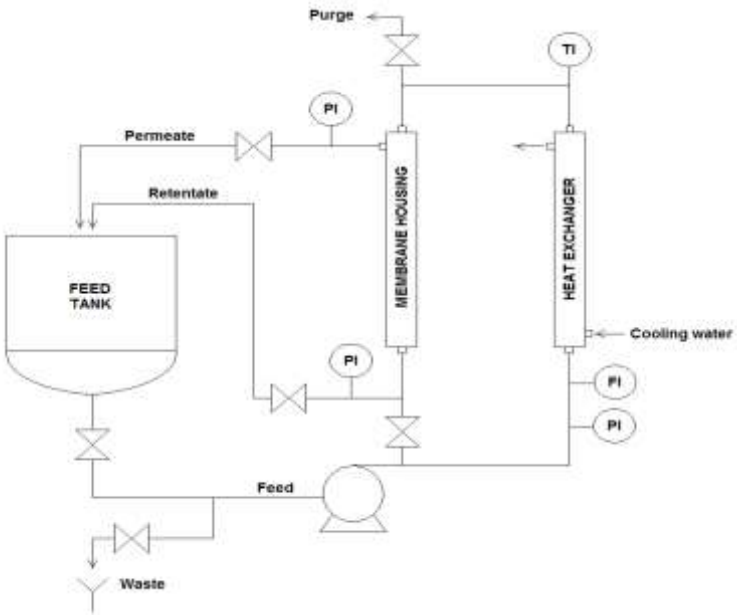

Figure 1. Microfiltration unit used in the laboratory.
(PI: pressure indicator; TI: temperature indicator; FI: flow indicator)

NF system at the laboratory scale

An Alfa Laval brand Pilot System 2.5″ RO/NF (Figure 2) was used as described in a previous work [24].

ISSN: 2277-9655
Impact Factor: 5.164
CODEN: IJESS7

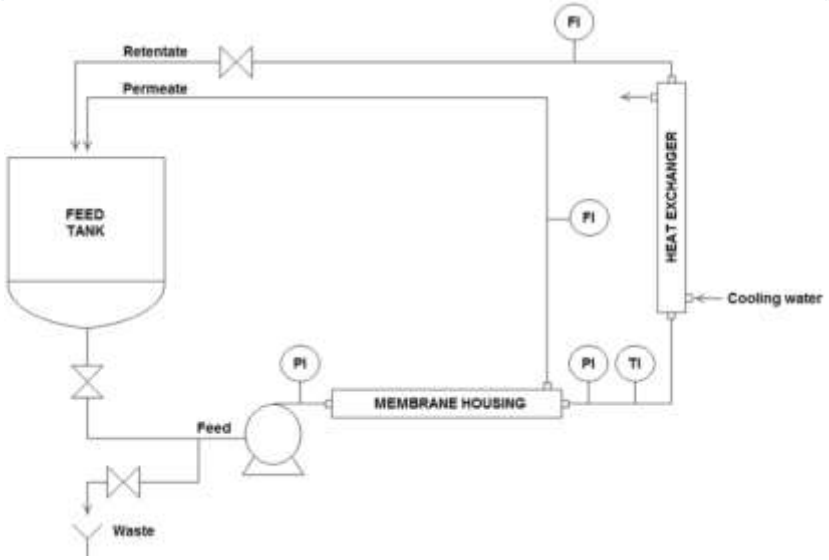

Figure 2. Diagram of the experimental NF/RO system.
(PI: pressure indicator; TI: temperature indicator; FI: flux indicator)

The Dow-Filmtec NF90–2540 membrane was evaluated. This membrane has an active surface of 2.6 m^2. Table 2 shows the hydraulic permeability and surface properties of the membrane. Hydraulic permeability was determined at 15 °C and Q_f = 750 L/h from the hydraulic curve [12].

Table 2. Surface roughness, porosity and hydraulic permeability of the membrane.

Membrane	Rejection-Size (%)	Hydraulic permeability, k_w (L/(m^2 h bar))	Roughness (nm) [25]	Porosity (%)[25]
NF90–2540	> 97 $MgSO_4$	4.2	27.75	16

Permeability was higher than that expected in RO membranes used in seawater desalination [26]. Permeability values for RO membranes in the working pressure range of 60–80 bar for seawater are between 0.1 and 0.8 L/(m^2 h bar) [25, 27].
A diagram of the operation using two-stage NF in a series is presented in Figure 3. The desalination system was test at a laboratory and pilot scale, with the MF (Figure 1) and NF units (Figure 2).

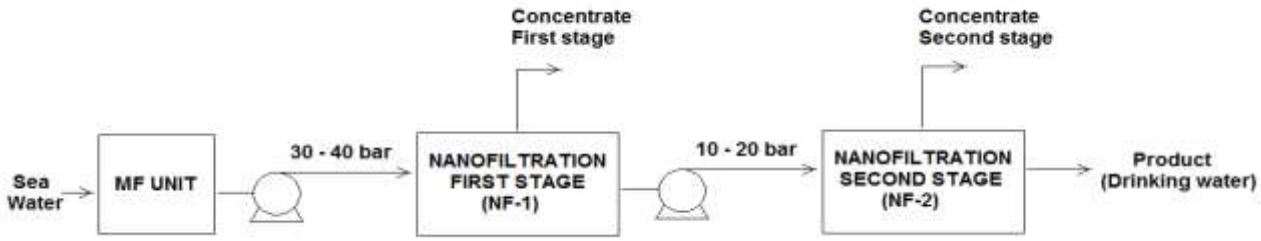

Figure 3. Scheme of the desalination system using two-stage nanofiltration in series.

For the first stage of nanofiltration, the operating conditions were as follows:

- Feed flow (Q_f): 875, 1250, and 1625 L/h.
- Pressure: 30, 34, 37, and 40 bar.
- Temperature: 15 °C.

The water produced from the first stage was stored in plastic drums at 4 °C until its subsequent use.
For the second stage of nanofiltration, the operating conditions were as follows:

- Feed flow (Q_f): 1625 L/h.
- Pressure: 10, 13, 16, and 20 bar.

ISSN: 2277-9655
Impact Factor: 5.164
CODEN: IJESS7

- Temperature: 15 °C.

Pilot system

A desalination pilot system was designed and operated based on data obtained at a laboratory scale. The system has a capacity to process up to 9 m^3/h of seawater.

As the system operates continuously, the pretreatment was a microfiltration stage (same as that at a laboratory scale), a stage that involves $FeCl_3$ dosing, and the subsequent removal of precipitates in prefiltering. A prefilter (Clack, model YTP2472–4) filled with commercial "clinoptilolite-zeolite" sand was used for precipitate removal. The MF cut off was 1-µm tubular filters (TwinPure, polyethylene).

Vitec–4000 antiscalant was used in the purification of seawater, while reverse osmosis was used as a desalination technique. The antiscalant was added continuously to reduce scaling formation. Dosage level was regulated to minimize fouling. After passing through the MF, turbidity values were lower than those recommended by the manufacturer of the NF90 membrane (DOW Chemical). Therefore, the input water met the quality requirements needed to ensure a safe and stable process.

Two modules were operated in parallel in both NF stages. Each module consisted of three membranes in the first stage and one membrane in the second stage. Only NF90–4040 membranes (7.6 m^2 active surface) were used. In the first NF stage, the system could be operated at a maximum pressure of 40 bar and was designed to reach a recovery between 20% and 25%. In the second NF stage, the system could be operated at a maximum pressure of 15 bar, reaching a recovery of 70% of permeate from the first stage.

Second-stage NF concentrate was directed back towards the seawater feed because it had low conductivity and turbidity. This recirculation was done in order to dilute fresh seawater and increase salt rejection in the first-stage NF, and also increase the recovery and use of the total water that entered the second stage. The product water, which conforms to the local standard NCh.409 for drinking water quality, was produced by partially mixing water generated in the first stage with that generated in the second stage.

Theory equations

The permeate water flux was calculated as:

$$J_w = \frac{\Delta V}{A_m \cdot \Delta t} \qquad (1)$$

Where $\Delta V/\Delta t$ is the permeate volume over time and A_m is the effective filtration area. The hydraulic permeability constant (k_w) was determined using the following expression:

$$k_w = \frac{J_w}{\Delta P} \qquad (2)$$

Where ΔP is operational pressure

Conductivity removal efficiency and ions removal efficiency of seawater was calculated using the expression given below:

$$R = \left(1 - \frac{C_p}{C_f}\right) \times 100 \qquad (3)$$

Where C_f is the conductivity or the heavy metal ions concentration of feed liquid, and C_p is the conductivities of the ions concentration of permeate liquid.

Finally, water recovery efficiency can be expressed as:

$$Y = \left(\frac{Q_p}{Q_f}\right) \times 100 \qquad (4)$$

Q_p is the amount of permeate (L/h) and Q_f is quatity of feed (L/h).

III. RESULTS AND DISCUSSION

Tests at the laboratory scale

Study of the NF90–2540 membrane in the first stage of NF

The permeate flux curves obtained for seawater present a significant reduction as compared to those for distilled water (Figure 4). The effects of the polarized layer increase at a greater salinity near the active layer of the membrane, decreasing the permeate flux [28, 29]. The k_w values were in the range of 1.2–1.3 L/(m^2 h bar) under all operating conditions, while membrane permeability experienced a reduction of about 70% compared to that observed when distilled water was filtered (Table 2). Water permeability increased around 10% at a greater feed velocity, thus resulting in greater permeate flux density. However, energy costs in feed pumping also increased by two-fold.

ISSN: 2277-9655
Impact Factor: 5.164
CODEN: IJESS7

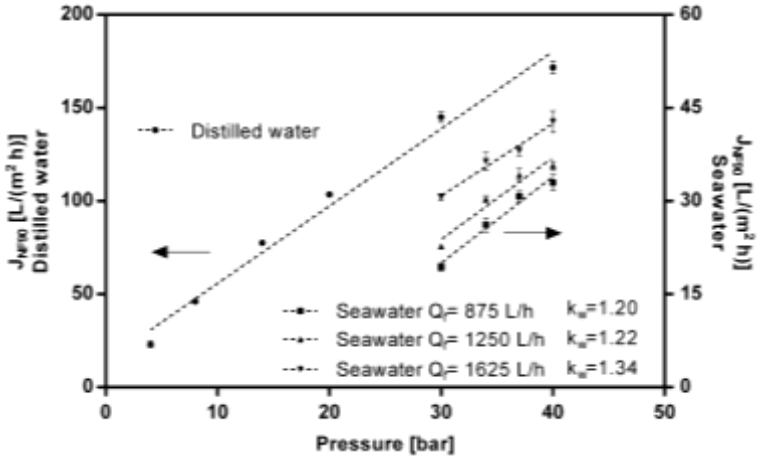

Figure 4. Permeate flux density using the NF90–2540 membrane at different pressures. Error bars represent 95% confidence interval of three measurements.

As observed in Figure 4, the linearity of the permeate flux is completely reduced once the pressure applied reaches 37 bar. This occurs because separation is controlled by mass-transfer mechanisms in the vicinity of the membrane surface. Such mechanisms are caused by the compaction of the polarized layer and increase in the osmotic pressure, thus resulting in membrane fouling, and causing flux reduction [30, 31]. This point is called 'critical flux' and refers to the maximum permeate flux that can be achieved by increasing the operating pressure, while maintaining linearity between permeate flux density and pressure [13]. It is known as the transition point from concentration polarization to fouling. As induced by pressure increase, it triggers adsorption of rejected solutes on the membrane surface, thus causing irreversible damage [30, 32].

In order to avoid membrane deterioration due to fouling, the optimal operating pressure of the first stage was set at 37 bar. A permeate flux of 39.7 L/(m^2 h) and a feed flow of 1625 L/h were obtained at this pressure.

An average increase of 35% was obtained in the permeate flux when the feed flow varied from 875 to 1625 L/h. In addition, the final permeate salinity also decreased, as indicated by electrical conductivity (Figure 5). The passage of water through the membrane increased when the feed flow was modified, whereas salt transport was maintained with the dilution of the permeate. However, salt concentration began to increase when reaching a certain critical pressure [13].

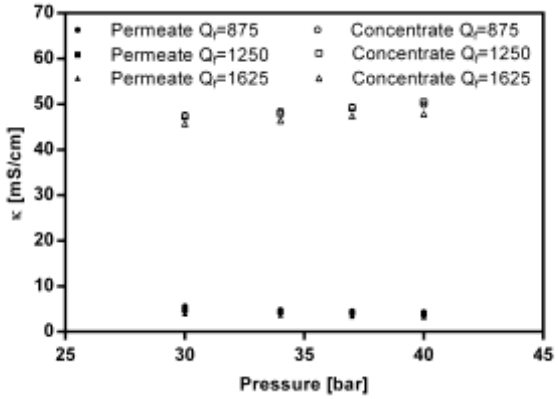

Figure 5. Electrical conductivity (κ) variation of permeate and concentrate with the operating pressure at different seawater feed flows. Error bars represent 95% confidence interval of three measurements.

The chemical analysis for the first-stage permeates is presented in Table 3.

ISSN: 2277-9655
Impact Factor: 5.164
CODEN: IJESS7

Table 3. Chemical analysis for first-stage permeates (NF90–2540 membrane; Q_f = 1625 L/h).

		Pressure (bar)					
		30	34	37	40		
Parameters	**Seawater**	**NF90 permeate**				**NCh. 409**	**WHO**
κ (μS/cm)	51100 ±100	3972 ±9	3684 ±25	3502 ±76	3332 ±91	-	-
NaCl (mg/L)	28150 ±63	2214 ±54	1850 ±47	1811 ±48	1770 ±61	-	-
Na^+ (mg/L)	11080 ±135	864 ±11	722 ±9	706 ±12	690 ±12	-	< 200*
Cl^- (mg/L)	19350 ±287	1362 ±46	1142 ±28	1120 ±39	1095 ±41	< 400	< 250*
Ca^{2+} (mg/L)	502 ±28	9.5 ±0.2	7.9 ±0.0	7.7 ±0.0	7.4 ±0.1	-	< 300*
Mg^{2+} (mg/L)	1672 ±37	23.9 ±4	19.7 ±4	19.3 ±3	18.5 ±7	< 125	
SO_4^{2+} (mg/L)	2719 ±46	N.D.	N.D.	N.D.	N.D.	< 500	< 500
TDS (mg/L)	35240 ±104	2252 ±23	1907 ±21	1875 ±19	1813 ±11	< 1500	< 1000
pH	7.4 ±0.3	7.2 ±0.2	7.3 ±0.3	7.2 ±0.3	7.2 ±0.2	6.5–8.5	6.5–8.5
R_{NaCl} (%)	-	92.1	93.4	93.6	93.7	-	

*: Recommended according to taste perception limits.

In the first stage, the separation obtained was high, achieving NaCl rejections of 93% when desalinating seawater. The obtained permeate did not meet the standards of the NCh.409 and the WHO for drinking water despite the above results (Table 3). Divalent ions were rejectedince NF90 is designed to retain more than 97% of $MgSO_4$ (Table 2). Therefore, the second stage of NF was necessary because concentrations of chloride and total dissolved solids (TDS) in the permeate were quite high.

Study of the NF90–2540 membrane in the second stage of NF

In the second stage of the process, the permeate obtained with the NF90–2540 in the first NF stage (1625 L/h) was used.

Salt concentration of the feed at the second stage was definitely lower than that of seawater. Similarly, the effects of osmotic pressure, viscosity, membrane fouling potential, and polarization were much smaller than in the first stage. On the other hand, permeate flux was high and operating pressures were low, thus resulting in a lower energy requirement than in the first stage [13, 26].

In the second stage of NF, the pressure sweep was carried out at 10–20 bar (Figure 6), indicating a significant decrease in pressure as compared to the first stage, NF_1. A flux density of 72.5 L/m^2 h was obtained at P = 16 bar. Therefore, the total system water recovery required to be increased in the NF_2 stage. In this stage, the permeability value was 4.12 L/(m^2 h bar). This was caused by the decrease in the concentration of salts from the salinity of the seawater (35,000 mg/L) to the salinity fed to the NF_2 stage (1875 mg/L), indicating an approximate total solid reduction of 95%.

ISSN: 2277-9655
Impact Factor: 5.164
CODEN: IJESS7

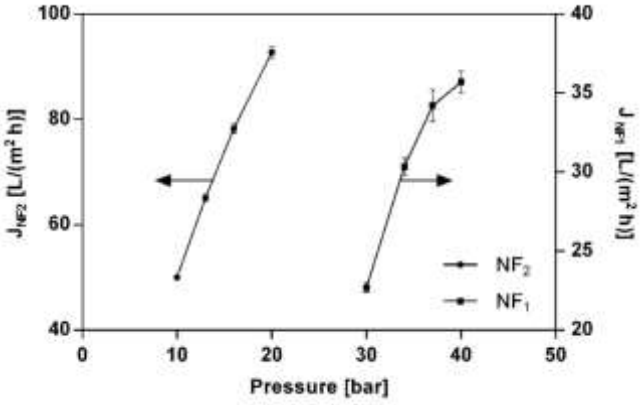

Figure 6. Permeate flux density obtained for the NF90–2540 membrane in stages NF_1 and NF_2 for a Q_f= 1625 L/h and at 15 °C. Error bars represent 95% confidence interval of three measurements.

The chemical analysis of the water generated in the second stage showed that water quality for the permeate of the second stage exceeded the standards provided by the NCh.409 and WHO for drinking water. NaCl retention was approximately 99% (Table 4).

Table 4. Chemical analysis for the second-stage (NF_2) permeates.

		Pressure (bar)					
		10	13	16	20		
Parameter	**Seawater**	**Stage NF2 permeate**				**NCh. 409**	**WHO**
κ (µS/cm)	51000 ±100	82.8 ±7	73.3 ±4	66.9 ±7	66.8 ±5	-	-
NaCl (mg/L)	28150 ±63	39.2 ±1	35.7 ±3	32.6 ±2	27.7 ±2	-	-
Na^+ (mg/L)	11080 ±135	15.3 ±0.9	13.9 ±0.8	12.7 ±1	10.9 ±0.5	-	< 200
Cl^- (mg/L)	19350 ±287	23.9 ±0.7	21.8 ±0.6	19.9 ±0.9	16.8 ±0.8	< 400	< 250
Ca^{2+} (mg/L)	502 ±28	0.12 ±0.03	0.1 ±0.02	0.1 ±0.01	0.08 ±0.01	-	< 300
Mg^{2+} (mg/L)	1672 ±37	0.31 ±0.03	0.25 ±0.02	0.25 ±0.03	0.2 ±0.03	< 125	
SO_4^{2+} (mg/L)	2719 ±46	N.D.	N.D.	N.D.	N.D.	< 500	< 500
TDS (mg/L)	35240 ±104	41.4 ±2	36.6 ±3	33.5 ±1	33.4 ±1	< 1500	< 1000
pH	7.4 ±0.3	6.8 ±0.1	6.7 ±0.1	6.8 ±0.1	6.8 ±0.2	6.5–8.5	6.5–8.5
R_{NaCl} (%)	-	97.8	98.0	98.2	98.5		
Total R_{NaCl} (%)	-	**99.8**	**99.87**	**99.88**	**99.9**		

The Mg^{2+} concentration, same as Ca^{2+}, was low due to the high polyvalent ion rejection of the NF membranes [10, 26]. For the NF90 membrane, it has already been reported that polyvalent ions show greater rejection as compared to monovalent ions (Na^+ and Cl^-) [14].

The data generated at laboratory scale was required to size a pilot system capable of generating between 1000 to 1500 L/h of drinking water from seawater.

Pilot plant assays

Effect of operating pressure in the first stage of NF (NF_1) at the pilot-plant scale

No clear deviation was observed from the linearity of the permeate flux with pressure at the pilot-plant scale. Therefore, 40 bar was the optimal working pressure to allow reaching a greater permeate flow in the NF_1 stage (Figure 7). The electrical consumption at P = 40 bar was 4 kWh/m^3, including the energy used for the pretreatment.

ISSN: 2277-9655
Impact Factor: 5.164
CODEN: IJESS7

This value was near the energy performance of current RO water desalination systems at the industrial scale (between 3.5 and 4 kWh/m^3), which uses high-performance energy recovery devices [33].

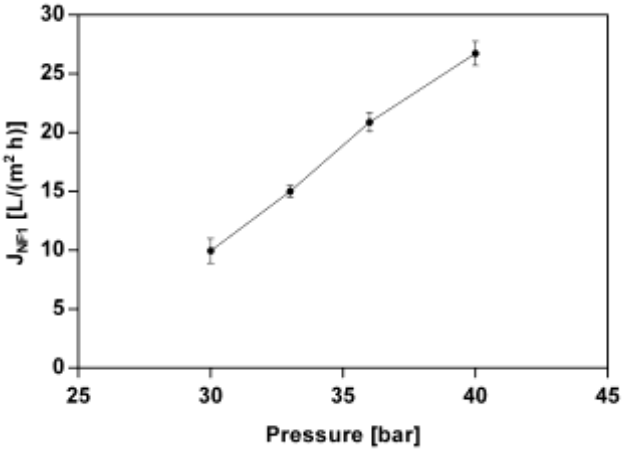

Figure 7. Permeate flux density variation as a function of first-stage (NF_1) pressure in the pilot plant (T = 18 °C; Q_f = 4.9 m^3/h; κ_f = 45.3 mS/cm). Error bars represent 95% confidence interval of three measurements.

The volumetric recovery of the generated water (Y_{NF1}) and total salt rejection (expressed in terms of conductivity) depend on TP (Figure 8). Total salt rejection increased as pressure increased, as observed for Na^+ and Cl^- ions with the use of the NF90 membrane by Liu et al. [14].

A greater amount of water permeates was observed as pressure increased from 84% at 30 bar to 91% at 36 bar, which affected salt rejection. The system recovery at 36 bar reached 20%. In the NF_1 stage, permeate conductivity was similar to that achieved by the experimental device at the laboratory scale.

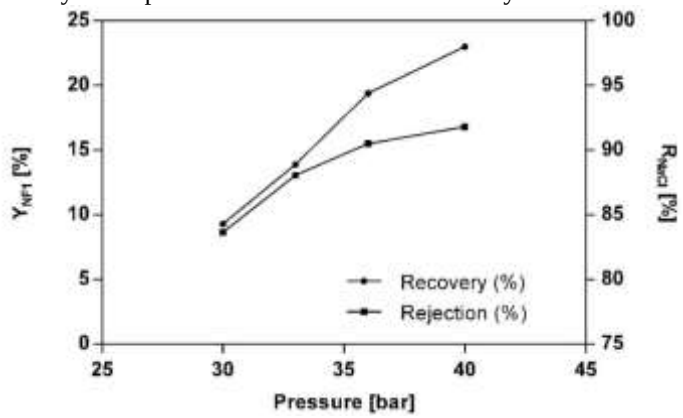

Figure 8. Variation of NaCl rejection (R_{NaCl}) and volumetric permeate recovery (Y_{NF1}) as a function of applied pressure at 18 °C and 4.9 m^3/h.

Effect of the operating pressure in the second stage of NF (NF_2) at the pilot-plant scale

In this stage, the concentrate was directed back into the seawater feed and diluted diluting it or fed back into the NF_2 stage. Permeate flux densities, conductivities, and volumetric permeate recovery obtained for the second-stage nanofiltration of the permeate generated in the first stage are presented in Table 5.

Table 5. Effect of operating pressure in the NF_2 stage at the pilot-plant scale on permeate flux density, conductivity and volumetric permeate recovery (NF_1 stage operated at: P = 40 bar; T = 17 °C).

P_{NF2} (bar)	κ_{NF1} (µS/cm)	κ_{NF2} (µS/cm)	J_{NF2} (L/m^2 h)	Y_{NF2} (%)	R_{NF2} (%)
10	3100 ±76	194 ±15	39.5 ±0.6	37	93.7
11	3500 ±73	183.2 ±19	45.8 ±0.7	57.8	94.8
12	3600 ±63	183 ±13	47.4 ±0.6	66.7	94.9
15	3800 ±81	178 ±10	51.3 ±0.5	83.4	95.3

ISSN: 2277-9655
Impact Factor: 5.164
CODEN: IJESS7

κ_{NF1}: Electrical conductivity of the permeate in the first stage of NF κ_{NF2}: Electrical conductivity of the permeate in the second stage of NF Q_{21}: Recirculated flow or concentrate, J_{NF2}: Permeate flux density in the second stage of NF Y_{NF2}: Volumetric permeate recovery in the second stage of NF and R_{NF1}: Salt rejection percentage in the second stage of NF.

In the NF_2 stage, permeate water qualities obtained were very high and fully meet local standards of the NCh.409 and the WHO guidelines for drinking water. When the nanofiltration modules were in series, the total energy consumption for both stages was 6 kWh/m^3 of product water, which is in the same order of magnitude of a reverse osmosis plant of a larger scale (3-7 kWh/m^3) [33, 34].
When the concentrate was directed back to the plant feed in the NF_2 stage, a decrease in the salt concentration of the feed (reflected in the initial conductivity) was observed. In turn, the recovery and quality in the NF_1 stage increased depending on the amount of NF_2 concentrate that was directed back to the feed. Feed conductivity decreased as concentrate recirculation increased, while the quality of the NF_1 permeate increased as conductivity decreased from 4 mS/cm to 3.5 mS/cm. At a pressure of 15 bar in the NF, the permeate flux density in the NF_1 stage (J_{11}) increased from 20.9 L/(m^2 h) to 22.4 L/(m^2 h). The permeate from the NF_1 stage increased to 27.0 L/(m^2 h) and the recovery of the NF_1 stage increased to 20.5% when recirculation was greater, i.e., 18 L/min at a pressure of 10 bar. Figure 9 shows the recovery of product water from the second stage in which an increase in the applied pressure was observed. Based on the measurement of the conductivity of the product water from the process, the total salt rejection was practically independent of the operating pressure of the second stage and was close to 99.5% (Figure 9). Therefore, this process can be considered as an alternative for seawater desalination because of high salt rejection. In order to achieve product water that complies with NCh.409 and the WHO guidelines, mixing permeate from NF_1 with permeate from NF_2 requires a greater volume of desalinated water to be produced.

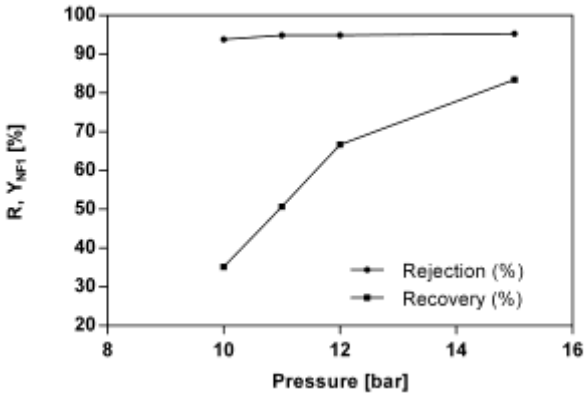

Figure 9. Variation of salt rejection R_{NaCl} (%) and volumetric permeate recovery Y_{NF1} (%) as a function of applied pressure in the second stage of NF.

Continuous pilot plant operation

In order to define the standard of the water produced in the pilot plant, optimal operating conditions in the first stage were determined based on the energy consumption under continuous operation. Afterwards, the variables that allow the greatest possible product flow at the lowest operational cost in the second stage of nanofiltration were also determined based on the specifications of NCh.409 and the WHO guidelines.
During the six months of continuous operation, characteristics of the seawater were maintained constant. Conductivity and pH values of the seawater used in this study are provided in Table 6.

Table 6. Chemical characterization of seawater.

κ_E (μS/cm)	51000 ±100
Ph	7.4 ±0.3

The variation in the feed pressure for NF_1 was studied during the continuous operation, keeping the rest of the operational variables constant.

ISSN: 2277-9655
Impact Factor: 5.164
CODEN: IJESS7

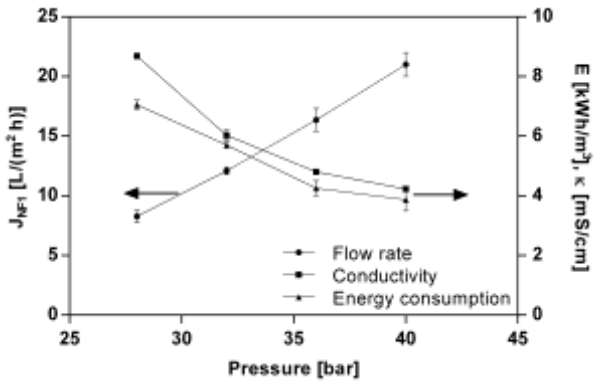

Figure 10. Effect of pressure on the permeate flow conductivity and energy consumption (E) in the first stage of nanofiltration. Error bars represent 95% confidence interval of three measurements.

As shown in Figure 10, as the motive power of the feed flow exceeds the osmotic pressure of the system [13] and the exerted TP affect the permeate flux [35]. A pressure of up to 40 bar was used as the maximum operating pressure of the NF90–2540 membranes. The diffusion and convection phenomena produced solute transport through a nanofiltration membrane. The process of convection prevailed over diffusion at greater pressures, thus increasing the permeate flux [25].

Electrical conductivity was measured at a one-hour interval in triplicate for the different working pressures in the pilot plant. Figure 10 shows the salt separation obtained in the first stage. It can be observed that the salt concentration of the permeate decreases with an increase in the pressure of the system [25]. No concentration polarization effects were observed at pressures near 40 bar, as already described in the literature [35]. At high pressures (36–40 bar), the permeate quality obtained with the membrane was within the expected range, and it was similar to that obtained at lower pressures in biologically treated water [36]. Moreover, tangential velocity also causes a decrease in electrical conductivity, thus preventing salt from compacting on the rough membrane and allowing better rejection [37].

The specific energy consumption of the first stage decreased with the applied pressure because the first stage was coupled with an energy recovery device, which uses the rejection energy of this stage to raise the feed pressure. Liu et al. [14] observed a similar trend in the two-stage nanofiltration in terms of the reduction in the specific energy consumption of the process with operational pressure.

Salt rejection in NF_1 was between 91 and 93% for sodium chloride and chloride ions, respectively (Table 7). Despite the high separation, the chemical analysis revealed that water composition did not comply with the Chilean standard NCh.409 and the WHO guidelines for drinking water quality. Therefore, the second stage of nanofiltration was necessary to achieve the required quality of the product.

Table 7. Salt concentrations and rejections in the first stage of nanofiltration.

Sample	**TDS** (mg/L)	**Cl^-** (mg/L)	**NaCl** (mg/L)	**pH**
Feed	35240 ±104	19350 ±287	28150 ±63	7.4 ±0.3
Permeate 1	2230 ±27	1350 ±24	2150 ±15	6.8 ±0.2
Standard NCh.409	<1500	<400	-	6.5–8.5
WHO	<1000	<250	-	6.5–8.5
% Rejected	93.65	93.02	91.04	-

In addition to the low specific energy consumption and the greater recovery rate of the NF_1 stage (22.5%), lower product water conductivity is achieved at a pressure of 40 bar (see Table 8).

Table 8. Chemical analysis of the first stage permeate with a recovery of 22.5%.

Parameter	Unit	Result
pH	-	6.8 ±0.2
Conductivity	µS/cm	4500 ±19

ISSN: 2277-9655
Impact Factor: 5.164
CODEN: IJESS7

Hardness	mg $CaCO_3$/L	245 ±5
Chloride	mg/L	1350 ±24
Sulfate	mg/L	5.7 ±0.7
Nitrate	mg/L	0.4 ±0.05
Boron	mg/L	1.45 ±0.15
Sodium	mg/L	2500 ±24
Magnesium	mg/L	24 ±3
Calcium	mg/L	10 ±1
Potassium	mg/L	125 ±9
Ammonium	µg/L	0
Carbonate	mg/L	0

Determination of the operating pressure in the second stage of NF operating continuously

The increase in the operating pressure resulted in an increase in the flow of produced water while operating independently in the NF_2 stage (Table 5). Figure 11 shows that an increase in the pressure in the second stage of nanofiltration produced an increase in the total water produced by the pilot plant during the continuous operation of the system.

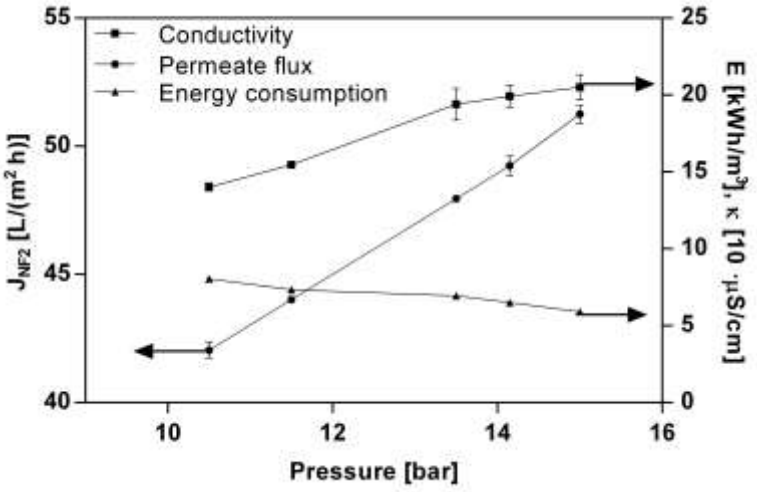

Figure 11. Effect of pressure on permeate flux density and conductivity in the second stage of nanofiltration. Error bars represent 95% confidence interval of three measurements.

The flow of the concentrate that returns to the feed decreased by increasing the permeate flux in the second stage of NF. Therefore, a greater salt load is received by the first stage of NF from the fresh seawater feed. Consequently, this caused an increase in the conductivity of the final product water generated by the plant as a result of the increased pressure applied in NF_2, as well as an increase in the flow of the produced water (Figure 11).

Table 9. Total monovalent salt rejection in the two-stage nanofiltration process.

Sample	TDS (mg/L)	Cl^- (mg/L)	NaCl (mg/L)	pH
Feed	35240 ±104	19350 ±287	28150 ±63	7.4 ±0.3
Permeate 1: 40 bar	2230 ±27	1350 ±24	2150 ±15	6.8 ±0.2
Permeate 2: 15 bar (Product water)	122 ±9	72 ±5	119 ±11	6.9 ±0.2
Nch.409 standard	<1500	<400	-	6.5–8.5

ISSN: 2277-9655
Impact Factor: 5.164
CODEN: IJESS7

WHO standard	<1000	<250	-	6.5–8.5
% First stage rejection	93.65	93.02	91.04	-
% Total rejection	99.65	99.63	99.50	-

Same as the total chemical analysis (Table 9), the microbiological analysis of this water also indicated that parameters did not meet the requirements set by the Chilean Standard NCh409 for drinking water quality (Table 10).

A significant reduction in boron concentration was observed in the product water (Table 11). In fact, seawater naturally contains an average concentration of 4.6 mg/L for this metalloid [38]. At a global level, various standards specify a maximum limit for boron though this parameter is not regulated by the Chilean standard NCh.409. For example, a limit of 1 mg/L is established by the EU [39]. The average boron concentration achieved by the pilot plant is below this limit as shown in Table 11. High boron concentrations have been observed in drinking water samples and urine samples of people in northern Chile [40].

Table 10. Microbiological analysis of the product water (Escherichia coli)

Entity	**Result (NMP/100 mL)**	**NCh. 409** [29]
Regional Health Service	< 1.0	< 5.0
External Analytical Laboratory 1	< 2.0	< 5.0
External Analytical Laboratory 2	< 3.0	< 5.0

Table 11. Chemical analysis of the product water.

Parameter	**Unit**	**Result**	**Maximum limit NCh. 409** [29]
True Color Pt-Co Scale	-	< 10	20.0
Odor	-	Odorless	Odorless
Taste	-	Tasteless	Tasteless
pH	-	6.9 ±0.2	6.5 < pH < 8.5
Conductivity	µS/cm	100 ±9	NA
Hardness	mg $CaCO_3$/L	2 ±0.3	NA
Fluoride	mg/L	<0.5	1.5
Chloride	mg/L	72 ±5	400.0
Sulfate	mg/L	0.2 ±0.03	500.0
Nitrate	mg/L	0.3 ±0.03	50.0
Nitrite	mg/L	< 0.1	3.0
Total Chrome	mg/L	< 0.05	0.05
Cadmium	mg/L	< 0.01	0.01
Cyanide	mg/L	< 0.05	0.05
Lead	mg/L	< 0.05	0.05
Selenium	mg/L	< 0.01	0.01
Arsenic	mg/L	0.003 ±0.002	0.01
Mercury	mg/L	< 0.001	0.001
Phosphorus	mg/L	0.36 ±0.02	NA
Iron	mg/L	0.00	0.3
Manganese	mg/L	0.00	0.1
Zinc	mg/L	0.00	3.0
Copper	mg/L	0.00	2.0

ISSN: 2277-9655
Impact Factor: 5.164
CODEN: IJESS7

Boron	mg/L	0.85 ±0.11	N.A.
Sodium	mg/L	30 ±2	NA
Magnesium	mg/L	0.4 ±0.08	125.0
Calcium	mg/L	0.4 ±0.09	NA
Potassium	mg/L	1.1 ±0.3	NA
Ammonium	µg/L	0	NA
Carbonate	mg/L	0	NA

NA: Not Applicable

Finally, the general economic assessment of the pilot plant process, which produces 25 m^3/day of drinking water, indicate that the drinking water is produced at a cost of US$ 0.75/m^3 (Table 12). As other reverse osmosis plants produce drinking water at a cost of US$ 1.9/m^3, the process using two-stage nanofiltration is very competitive [41, 42]. Furthermore, the reverse osmosis process generates highly pure water as a product, which requires to be remineralized. However, nanofiltration also allows the formulation of water for special purposes other than drinking, e.g., water from the first nanofiltration stage can be used for personal cleanliness, toilet flushing, laundry or irrigation. In addition, nanofiltration allows for the production of water with different specifications since it works in two stages with variable operating conditions.

Table 12. Costs associated with production in the pilot plant

TYPE OF SYSTEM	NANOFILTRATION PLANT	AVERAGE IN REVERSE OSMOSIS PLANTS
WATER PRODUCTION INPUT		
Daily Water Production (m^3)	25	50
VARIABLE COSTS		
Energy cost (%)	53.8	57.0
Chemicals (%)	7.7	9.6
Subtotal (%)	61.5	66.6
FIXED COST		
Membrane Replacement (%)	18.2	9.5
Maintenance and labor (%)	20.3	23.9
Subtotal (%)	38.5	33.4
Cost of Water Production (US$/$m^3$)	0.75	1.89[41, 42]

IV. CONCLUSION

At the laboratory scale, the NF90 membrane in the first stage presented a permeate flux density of 39.7 L/m^2h at P = 37 bar, Q_f = 1625 L/h, seawater temperature of 14-18 °C and a high rejection of NaCl, i.e., 93.6% on average. The NF90 membrane in the second stage delivered a permeate flux of 72.5 L/m^2h and a salt rejection of 99% at 16 bar (with respect to the NF_1 stage), achieving a product that meets Chilean and international standards (WHO) for drinking water quality. This indicates that water can be used in both stages.

At the pilot scale, a permeate flux density of 21.0 L/m^2 h with a recovery of 22.5% for a feed flow of 4.9 m^3/h at 40 bar was achieved in the first stage, while the salt rejection reached 91%. In the second stage of NF at P = 15 bar, the permeate flow was 51.3 L/m^2 h, reaching a total system recovery of 24% and a total salt rejection of 99.6%, which complies with the specifications of the Chilean standard NCh.409 and the WHO guidelines. The final permeate contains 118 mg/L of NaCl.

Microbiological and chemical analyses were carried out to confirm the absence of total fecal coliform and *Escherichia coli*, and a low concentration of boron, salts, and minerals in the product water. The implemented pilot plant is capable of producing 25 m^3/day of drinking water with operating costs of US$0.75/$m^3$. Total electrical consumption represents approximately 53.8% of the operating costs of the plant. Furthermore, the low

operating pressure used in nanofiltration results in costs that are much lower than those of the alternative provisions used, such as RO water desalination systems (US$1.89/$m^3$).

V. ACKNOWLEDGEMENTS

This study was funded by CONICYT/FONDAP Grant 15130015.

VI. REFERENCES

1. R.I. McDonald, P. Green, D. Balk, B.M. Fekete, C. Revenga, M. Todd, M. Montgomery, Urban growth, climate change, and freshwater availability, Proc. Natl. Acad. Sci., 108 (2011) 6312-6317.
2. X. Zhao, R. Zhang, Y. Liu, M. He, Y. Su, C. Gao, Z. Jiang, Antifouling membrane surface construction: Chemistry plays a critical role, J. Membr. Sci., 551 (2018) 145-171.
3. H. March, The politics, geography, and economics of desalination: a critical review, WIREs Water, 2 (2015) 231-243.
4. P.S. Goh, W.J. Lau, M.H.D. Othman, A.F. Ismail, Membrane fouling in desalination and its mitigation strategies, Desalination, 425 (2018) 130-155.
5. N.R. Council, Desalination: A National Perspective, The National Academies Press, Washington, DC, 2008.
6. G.W. Intelligence, Water Desalination Report in, 2015.
7. M. Liu, S. Yu, J. Tao, C. Gao, Preparation, structure characteristics and separation properties of thin-film composite polyamide-urethane seawater reverse osmosis membrane, J. Membr. Sci., 325 (2008) 947-956.
8. A.L. Ahmad, B.S. Ooi, A. Wahab Mohammad, J.P. Choudhury, Development of a highly hydrophilic nanofiltration membrane for desalination and water treatment, Desalination, 168 (2004) 215-221.
9. A.W. Mohammad, Y.H. Teow, W.L. Ang, Y.T. Chung, D.L. Oatley-Radcliffe, N. Hilal, Nanofiltration membranes review: Recent advances and future prospects, Desalination, 356 (2015) 226-254.
10. D. Zhou, L. Zhu, Y. Fu, M. Zhu, L. Xue, Development of lower cost seawater desalination processes using nanofiltration technologies — A review, Desalination, 376 (2015) 109-116.
11. X. Lu, X. Bian, L. Shi, Preparation and characterization of NF composite membrane, J. Membr. Sci., 210 (2002) 3-11.
12. D.L. Oatley-Radcliffe, S.R. Williams, M.S. Barrow, P.M. Williams, Critical appraisal of current nanofiltration modelling strategies for seawater desalination and further insights on dielectric exclusion, Desalination, 343 (2014) 154-161.
13. Y.A.L. Gouellec, A Novel Approach to Seawater Desalination Using Dual-Staged Nanofiltration, IWA Publishing, 2007.
14. M. Liu, C. Zhou, B. Dong, Z. Wu, L. Wang, S. Yu, C. Gao, Enhancing the permselectivity of thin-film composite poly(vinyl alcohol) (PVA) nanofiltration membrane by incorporating poly(sodium-p-styrene-sulfonate) (PSSNa), J. Membr. Sci., 463 (2014) 173-182.
15. M. Ernst, A. Bismarck, J. Springer, M. Jekel, Zeta-potential and rejection rates of a polyethersulfone nanofiltration membrane in single salt solutions, J. Membr. Sci., 165 (2000) 251-259.
16. A.E. Childress, M. Elimelech, Effect of solution chemistry on the surface charge of polymeric reverse osmosis and nanofiltration membranes, J. Membr. Sci., 119 (1996) 253-268.
17. M.D. Afonso, R.B. Yan˜ez, Nanofiltration of wastewater from the fishmeal industry, Desalination, 139 (2001) 429.
18. D. Vial, G. Doussau, The use of microfiltration membranes for seawater pre-treatment prior to reverse osmosis membranes, Desalination, 153 (2003) 141-147.
19. I.N.D.N. (CHILE), Agua Potable – Parte 1: Requisitos., in: NCH409/1: Of 2005, Santiago, Chile, 2005, pp. 13.
20. D. Aitken, D. Rivera, A. Godoy-Faúndez, E. Holzapfel, Water Scarcity and the Impact of the Mining and Agricultural Sectors in Chile, Sustainability, 8 (2016) 128.
21. B.J. P., R. Roberto, G.R. D., M. Francisca, Anthropogenic and natural contributions to the Southeast Pacific precipitation decline and recent megadrought in central Chile, Geophysical Research Letters, 43 (2016) 413-421.
22. E.W. Rice, L. Bridgewater, A.P.H. Association, A.W.W. Association, W.E. Federation, Standard Methods for the Examination of Water and Wastewater, American Public Health Association, 2012.

ISSN: 2277-9655
Impact Factor: 5.164
CODEN: IJESS7

23. M.D. Afonso, J.O. Jaber, M.S. Mohsen, Brackish groundwater treatment by reverse osmosis in Jordan, Desalination, 164 (2004) 157-171.
24. R. Bórquez, J. Ferrer, Seawater desalination by combined nanofiltration and ionic exchange, Desal. Water Treat., 57 (2016) 28122-28132.
25. N. Hilal, H. Al-Zoubi, A.W. Mohammad, N.A. Darwish, Nanofiltration of highly concentrated salt solutions up to seawater salinity, Desalination, 184 (2005) 315-326.
26. A. AlTaee, A.O. Sharif, Alternative design to dual stage NF seawater desalination using high rejection brackish water membranes, Desalination, 273 (2011) 391-397.
27. A. Subramani, E.M.V. Hoek, Biofilm formation, cleaning, re-formation on polyamide composite membranes, Desalination, 257 (2010) 73-79
28. M.F.A. Goosen, S.S. Sablani, S.S. Al-Maskari, R.H. Al-Belushi, M. Wilf, Effect of feed temperature on permeate flux and mass transfer coefficient in spiral-wound reverse osmosis systems, Desalination, 144 (2002) 367-372.
29. R. Wang, Y. Li, J. Wang, G. You, C. Cai, B.H. Chen, Modeling the permeate flux and rejection of nanofiltration membrane separation with high concentration uncharged aqueous solutions, Desalination, 299 (2012) 44-49.
30. C.Y. Tang, T.H. Chong, A.G. Fane, Colloidal interactions and fouling of NF and RO membranes: A review, Adv. Colloid Interface Sci., 164 (2011) 126-143.
31. R.W. Baker, Membrane Technology and Applications, Wiley, 2012.
32. P. Bacchin, P. Aimar, R.W. Field, Critical and sustainable fluxes: Theory, experiments and applications, J. Membr. Sci., 281 (2006) 42-69.
33. N. Ghaffour, T.M. Missimer, G.L. Amy, Technical review and evaluation of the economics of water desalination: Current and future challenges for better water supply sustainability, Desalination, 309 (2013) 197-207.
34. D.L. Shaffer, N.Y. Yip, J. Gilron, M. Elimelech, Seawater desalination for agriculture by integrated forward and reverse osmosis: Improved product water quality for potentially less energy, J. Membr. Sci., 415-416 (2012) 1-8.
35. L.G. Peeva, E. Gibbins, S.S. Luthra, L.S. White, R.P. Stateva, A.G. Livingston, Effect of concentration polarisation and osmotic pressure on flux in organic solvent nanofiltration, J. Membr. Sci., 236 (2004) 121-136.
36. S. Bunani, E. Yörükoğlu, G. Sert, Ü. Yüksel, M. Yüksel, N. Kabay, Application of nanofiltration for reuse of municipal wastewater and quality analysis of product water, Desalination, 315 (2013) 33-36.
37. M. Mänttäri, A. Pihlajamäki, M. Nyström, Comparison of nanofiltration and tight ultrafiltration membranes in the filtration of paper mill process water, Desalination, 149 (2002) 131-136.
38. K.L. Tu, L.D. Nghiem, A.R. Chivas, Boron removal by reverse osmosis membranes in seawater desalination applications, Sep. Purif. Technol., 75 (2010) 87-101.
39. C.o.t.E. Union, Council Directive 98/83/EC, in: On the quality of water intended for human consumption, 1998.
40. S. Cortes, E. Reynaga-Delgado, A.M. Sancha, C. Ferreccio, Boron exposure assessment using drinking water and urine in the North of Chile, Sci Total Environ, 410-411 (2011) 96-101.
41. I.C. Karagiannis, P.G. Soldatos, Water desalination cost literature: review and assessment, Desalination, 223 (2008) 448-456.
42. M. Sarai Atab, A.J. Smallbone, A.P. Roskilly, An operational and economic study of a reverse osmosis desalination system for potable water and land irrigation, Desalination, 397 (2016) 174-184.